

Research Article

Inherent Directionality Determines Spatial Release from Masking at the Tympanum in a Vertebrate with Internally Coupled Ears

MICHAEL S. CALDWELL,^{1,2} NORMAN LEE,¹ AND MARK A. BEE^{1,3}

¹*Department of Ecology, Evolution, and Behavior, University of Minnesota, 140 Gortner Laboratory, 1479 Gortner Ave, St. Paul, MN 55108, USA*

²*Present Address Department of Biology, Gettysburg College, McCreary Hall, 300 North Washington St, Gettysburg, PA 17325, USA*

³*Graduate Program in Neuroscience, University of Minnesota, 140 Gortner Laboratory, 1479 Gortner Ave, St. Paul, MN 55108, USA*

Received: 22 July 2015; Accepted: 10 April 2016; Online publication: 28 April 2016

ABSTRACT

In contrast to humans and other mammals, many animals have internally coupled ears that function as inherently directional pressure-gradient receivers. Two important but unanswered questions are to what extent and how do animals with such ears exploit spatial cues in the perceptual analysis of noisy and complex acoustic scenes? This study of Cope's gray treefrog (*Hyla chrysoscelis*) investigated how the inherent directionality of internally coupled ears contributes to spatial release from masking. We used laser vibrometry and signal detection theory to determine the threshold signal-to-noise ratio at which the tympanum's response to vocalizations could be reliably detected in noise. Thresholds were determined as a function of signal location, noise location, and signal-noise separation. Vocalizations were broadcast from one of three azimuthal locations: frontal (0°), to the right (+90°), and to the left (−90°). Masking noise was broadcast from each of 12 azimuthal angles around the frog (0 to 330°, 30° separation). Variation in the position of the noise source resulted in, on average, 4 dB of spatial release from masking relative to co-located conditions. However, detection thresholds could be up to 9 dB lower in the “best ear for

listening” compared to the other ear. The pattern and magnitude of spatial release from masking were well predicted by the tympanum's inherent directionality. We discuss how the magnitude of masking release observed in the tympanum's response to spatially separated signals and noise relates to that observed in previous behavioral and neurophysiological studies of frog hearing and communication.

Keywords: acoustic communication, cocktail party problem, pressure-gradient receiver, sound source segregation, spatial unmasking, vocal communication

INTRODUCTION

In crowded social environments, overcoming the effects of noise and acoustic clutter represents a fundamental communication problem for humans (McDermott 2009) and for many other animals (Bee and Micheyl 2008; Brumm 2013; Wiley 2015). Spatial separation in azimuth between signals of interest and sources of noise or other concurrent sounds can lead to marked improvements in signal detection and recognition. This phenomenon, termed “spatial release from masking” (SRM), has been most thoroughly investigated in humans, for which separating a source of speech from sources of speech-shaped noise

Correspondence to: Mark A. Bee · Department of Ecology, Evolution, and Behavior · University of Minnesota · 140 Gortner Laboratory, 1479 Gortner Ave, St. Paul, MN 55108, USA. Telephone: ++1-612-624-6749; email: mbee@umn.edu

or other speech sounds can significantly improve speech intelligibility (reviewed in Bronkhorst 2000).

At least two mechanisms—one monaural and the other binaural—contribute to SRM in humans (Bronkhorst and Plomp 1988; Zurek 1992). First, compared with signals and noise that originate from the same location, spatial separation in azimuth results in a higher signal-to-noise ratio (SNR) at one of the two ears due to the sound shadow created by the head. Thus, at the periphery, a monaural cue exists at the ear with the higher SNR, making it the so-called best ear for listening. Second, when signals and noise originate from the same location, there are no interaural disparities in their arrival times or intensities at the two ears. But when they originate from different locations in azimuth, there are differences in the binaural cues each produces. The central nervous system contributes to masking release through binaural processing of these disparities.

Humans are not the only animals that experience SRM. This and related perceptual phenomena, and their neural correlates, have been investigated in a diversity of other mammals, such as mice (Ison and Agrawal 1998), ferrets (Hine et al. 1994), cats (Caird et al. 1989), pinnipeds (Holt and Schusterman 2007), and bats (Warnecke et al. 2014), as well as in crickets (Schmidt and Römer 2011), frogs (Schwartz and Gerhardt 1989), and songbirds (Dent et al. 2009). The wide diversity of animals that experience SRM presents fruitful opportunities to investigate potential evolutionary diversity in its underlying physiological mechanisms.

In contrast to mammals, non-mammalian tetrapods, as well as many insects, have internally coupled ears (Gerhardt and Huber 2002; Christensen-Dalsgaard 2005, 2011; Robert 2005; Michelsen and Larsen 2008; Römer 2015). Whereas each ear of a mammal functions independently as a pressure receiver, ears that are internally coupled can function as pressure-gradient receivers. Because sounds impinge on both sides of the tympana, pressure-gradient ears are also directional, typically exhibiting cardioid patterns of directional sensitivity that are bilaterally symmetrical about the midline (Ho and Narins 2006). Precisely how the inherent directionality of internally coupled ears contributes to SRM has not been formally investigated.

The present study investigated how the amplitude of tympanum vibrations in Cope's gray treefrog (*Hyla chrysoscelis*) varies in the presence of signals (vocalizations) and noise that were either co-located or spatially separated in azimuth. Gray treefrogs have a well-described vocal communication system (reviewed in Gerhardt 2001) and have been the subjects of behavioral studies of sound localization and SRM, as well as biophysical studies of directional hearing

(reviewed in Bee 2015). Males produce pulsatile advertisement calls (Fig. 1A) to attract females in breeding choruses that are often dense and characterized by high levels of background noise. Females experience SRM that is manifest in shorter response latencies, lower signal recognition thresholds, and improved signal discrimination. The directionality of the tympanum's response to sound exhibits the well-known cardioid response typical of pressure-gradient receivers.

We tested the hypothesis that the inherent directionality of the internally coupled ears determines the patterns and magnitude of SRM in the amplitude of the tympanum's response to signals presented in noise. Using laser vibrometry and signal detection theory, we measured the threshold SNR at which the tympanum responded to a synthetic advertisement call (Fig. 1A) presented in noise having a frequency spectrum and overall level typical of natural gray treefrog choruses (Nityananda and Bee 2011; Caldwell and Bee, unpublished data). Thresholds were measured at three signal locations (Fig. 1B; frontal, 0°; to the right, +90°; to the left, -90°). For each signal location, the location of the noise was manipulated across 12 different sound incidence angles around the animal (0 to 330°, in 30° steps). This factorial design allowed us to determine detection thresholds and SRM as functions of absolute signal location, absolute noise location, and relative spatial separation between signal and noise.

MATERIALS AND METHODS

All of our procedures followed the *Guide for the Care and Use of Laboratory Animals* and were approved by the University of Minnesota's Institutional Animal Care and Use Committee (protocol no. 1103A97192).

Subjects

We recorded responses from 17 Cope's gray treefrogs (nine male, eight female) of the western mtDNA lineage (Ptacek et al. 1994). We collected animals during June and July 2013, from wetlands in Carver, Hennepin, and Wright counties, Minnesota, USA. Animals were housed in terraria equipped with sphagnum moss, perches, shelter, broad-spectrum lighting, and filtered flow-through water (Aquaneering Inc., San Diego, CA). Each subject's body mass (to the nearest 0.1 g), body length (snout-to-vent length, to the nearest 0.1 mm), and interaural distance (to the nearest 0.1 mm) were measured just prior to making tympanum recordings using a digital balance and dial calipers. There were no significant sex differences in mean (\pm SD) mass ($t_{15}=0.33$, $P=0.747$; females, 4.8 ± 1.1 g; males, 4.6 ± 1.1 g), length

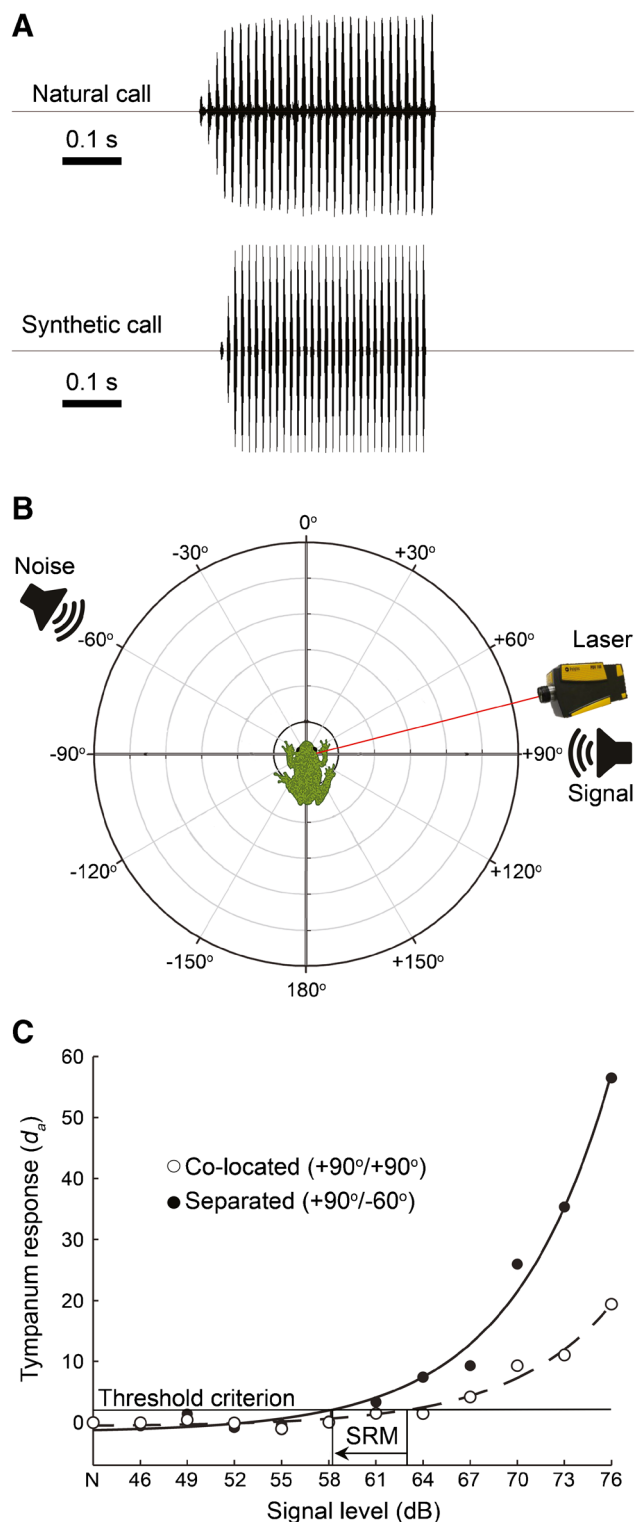
FIG. 1. Measuring signal detection thresholds for the tympanum's response to advertisement calls presented in chorus-like noise. **A** Waveforms depicting a natural advertisement call of *Hyla chrysoscelis* (top) and the synthetic call (bottom) used in the present study. The amplitudes of both calls have been normalized to the same value; scale bars indicate time. **B** Schematic illustration of the spatial arrangements of signals and noise in azimuth relative to a subject and the measurement laser. Signals were broadcast from one of three positions relative to the subject's snout (0, +90, and -90°). Noise was presented from 12 locations around the animal separated by 30° (e.g., 0, +30, +60°, etc.). The configuration illustrated here includes a signal location of +90° and a noise location of -60° (+90/-60°). The laser for measurement was positioned at approximately +75°. Objects in this schematic are not drawn to scale. **C** Data from one animal (mhch041) showing computed d_a values with fitted exponential fits as a function of signal level for a co-located condition (open circles and dashed line, +90/+90°) and a separated condition (closed circles and solid line, +90/-60°). The solid horizontal line depicts the threshold criterion ($d_a=2$), and the vertical dashed lines indicate the signal levels at which the two fitted exponential curves cross the threshold criterion. The threshold difference between the two vertical lines corresponds to the magnitude of spatial release from masking (SRM).

($t_{15}=1.22$, $P=0.240$; females, 37.1 ± 2.1 mm; males, 36.0 ± 1.6 mm), or interaural distance ($t_{15}=1.06$, $P=0.306$; females, 12.7 ± 0.6 mm; males, 12.3 ± 0.9 mm).

To make stable tympanum recordings, we immobilized each subject with an intramuscular injection of d-tubocurarine chloride (1 $\mu\text{g/g}$). Anurans can receive acoustic input not only through their tympana but also through the body wall and lungs, as beautifully illustrated in Narins (1995). The acoustic coupling between the lungs, mouth cavity, and middle ears influences the frequency response and directionality of tympanum vibrations (Ehret et al. 1990; Jørgensen 1991; Jørgensen et al. 1991; Caldwell et al. 2014). Therefore, we allowed subjects to regulate their own lung volume as the immobilizing agent took effect. The extent of lung inflation (assessed by examining body wall extension) resembled that observed for unmanipulated treefrogs sitting in a natural posture. Previous studies using similar methodology found no significant change in apparent lung air volume during the course of a recording session (Caldwell et al. 2014). A typical recording session lasted approximately 2 h. Following a recording session, subjects received intramuscular injections of edrophonium chloride (3 $\mu\text{g/g}$) to facilitate recovery from the immobilizing agent.

Tympanum Measurements and Acoustic Stimulation

We measured the amplitude response of the tympanum using a laser vibrometer (PDV-100, Polytec, Irvine, CA). A previous study of ear mechanics in this



species indicated that directional information is carried primarily by the amplitude response of the tympanum, with the phase of tympanum vibrations exhibiting little variation as sound incidence angle

changes (Caldwell et al. 2014). Measurements were made in a custom-built, semi-anechoic sound chamber (2.9 m × 2.7 m × 1.9 m, $L \times W \times H$, inside dimensions; Industrial Acoustics Company, Bronx, NY). The floor of the sound chamber was carpeted, and its walls and ceiling were lined with acoustic foam (Sonex, model VLW-60; Pinta Acoustic, Inc., Minneapolis, MN). We placed subjects atop a 30-cm tall pedestal made from acoustically transparent wire mesh (0.9-mm-diameter wire, 10.0-mm grid spacing), and we positioned the top of the pedestal 120 cm above the chamber floor using a horizontal, 70-cm-long, metal beam. The support beam was attached to a vibration isolation table (Technical Manufacturing Corporation, Peabody, MA). Both the beam and table were covered in acoustic foam. The tip of the subject's lower jaw was kept parallel to the floor of the chamber and rested on an arch of thin metal wire, such that the subject was positioned in a natural sitting posture with a raised head that was in line with its body.

Acoustic stimuli were presented from two speakers (Mod1, Orb Audio, New York, NY) positioned 50 cm away from the center of the subject's head, measured along the interaural axis (i.e., an imaginary line connecting the centers of both tympana). Each speaker was attached to a separate rotating arm made from 2.1-cm-diameter metal tubing covered with acoustic foam and suspended from the ceiling of the chamber. This apparatus allowed us to position each speaker at any azimuthal angle relative to the orientation of the stationary subject's snout while maintaining a fixed distance from the center of the head along the interaural axis (Fig. 1B). Custom software (Stimprog v. 5.42) written in MATLAB (v.2011a, MathWorks, Natick, MA) controlled a digital and analogue interface (NI USB 6259, National Instruments, Austin, TX) for stimulus presentation and recording. Signal levels were adjusted with a programmable attenuator (PA5, Tucker-Davis Technologies, Alachua, FL) connected to a power amplifier (Sonamp 1230, Sonance, San Clemente, CA).

The side of the animal from which measurements were taken (right) was considered the ipsilateral side. Sound presentation angles on the ipsilateral side are here indicated by positive values, and negative sound presentation angles indicate that the speaker was on the contralateral (left) side of the animal. Thus, +90° describes a location directed toward the ipsilateral ear, -90° a location directed toward the contralateral ear, and 0° a location directly in front of the frog's snout (see Fig. 1B).

Prior to recording, the opening to each Eustachian tube inside the mouth cavity was visually inspected to ensure that it was free from obstruction and was swabbed using a lint-free wipe to clear away any mucus. During our recordings, the mouth cavity was closed. We

placed a small (45–63 μm diameter) retroreflective glass bead (P-RETRO-500, Polytec, Irvine, CA) on the center of the ipsilateral tympanum of each subject to enhance the reflectance of the membrane. We focused the laser vibrometer on the bead. The vibrometer was mounted to the vibration isolation table and positioned at approximately +75° relative to the orientation of the subject's snout, such that the speakers never obstructed the laser beam during data collection. A probe microphone (40SC, G.R.A.S., Holte, Denmark) was positioned with the probe tip located approximately 2 mm rostral to the edge of the ipsilateral tympanum. Microphone gain was increased using a battery-powered amplifier (MP-1, Sound Devices, Reedsburg, WI).

The signal consisted of a synthetic *H. chrysoscelis* advertisement call with spectral and temporal properties based on the average values of calls recorded at our field sites in Minnesota (Fig. 1A; see Ward et al. 2013b, for additional information on call synthesis). Each call (590 ms total duration) was composed of 30 pulses shaped with a species-typical amplitude envelope and having harmonically related spectral components at frequencies (and relative amplitudes) of 1250 Hz (-9 dB) and 2500 Hz (0 dB). Signals were presented as a sequence of 11 calls (1 call/s) that increased sequentially in sound pressure level between 46 and 76 dB SPL (re 20 μPa) in 3-dB steps. On different testing days, this signal sequence was broadcast from one of three randomly selected locations (0, +90, or -90°). For each signal location tested on a given day, noise was presented at each of 12 locations in azimuth (0, +30, +60, +90, +120, +150, +180, -150, -120, -90, -60, and -30°). The initial noise location was selected randomly, and subsequent noise locations were tested in order of increasing consecutive angle (e.g., -60, -30, 0, +30°, etc.). The noise was artificial and consisted of white noise that was band-limited (500 to 4500 Hz) and broadcast at 79 dB SPL (43 dB spectrum level), beginning 2 s before the first call and ending immediately after the 11th and final call in the signal sequence. The 2 s of noise preceding the first call in the sequence allowed us to measure the tympanum's response to noise alone. The sound pressure level and frequency content of our artificial noise were chosen to be representative of natural background noise at breeding ponds in Minnesota (Nityananda and Bee 2011; Caldwell and Bee, unpublished data). A different token of band-limited noise was used in each testing session for each subject, but the same token was presented at all locations within a testing session. Signals and noise were presented from separate speakers, except during the three co-located conditions (signal/noise, 0/0°; +90/+90°; and -90/-90°), in which they were presented from the same speaker. The signal sequence and concurrent noise were presented three times at each combination of signal and noise location. At the completion of all recordings, each

subject's right tympanum had been measured three times in response to noise alone and in response to signals in noise at 11 different signal levels, at each of 36 combinations of 3 signal locations and 12 noise locations.

To account for frequency filtering introduced by the sound presentation equipment and spatial variation in room acoustics within the sound chamber, separate equalization filters were produced once per testing session for all 12 speaker positions using the custom-written software. Equalized signals and noises deviated no more than ± 1 dB from the target amplitude across their full frequency range. The absolute amplitudes of signals and noises were calibrated before each subject was placed in the chamber using a sound level meter (type 2250, Brüel & Kjær Inc. North America, Norcross, GA) with its microphone (type 4189) suspended by an extension cable (10 m in total length) from the ceiling of the sound chamber and positioned in the same location where the center of a subject's head would be during a recording. As we have previously reported, our playback speakers exhibit little in the way of harmonic distortion across the frequencies and levels used in the present study (e.g., percent harmonic distortion of 0.9 % reported in Buerkle et al. 2014). At the moderate signal levels used in the present study, harmonics above the spectral components present in the signal had relative amplitudes that were 50 to 60 dB lower, if they appeared above the noise floor at all.

Threshold Determination

Digital recordings (48 kHz, 16-bit) of tympanum vibrations and sound pressure adjacent to the tympanum were analyzed in MATLAB. We determined the mean and variance of the RMS amplitudes recorded over the three presentations of each call in the signal sequence at each noise location. During the first 2 s of each stimulus presentation, we also determined the mean and variance of the RMS amplitude recorded over three segments of noise alone, each equivalent to the duration of the call. As an index of the detectability of the signal in noise (Simpson and Fitter 1973), we calculated the d_a value for each signal amplitude at each combination of signal location and noise location as

$$d_a = \frac{(\mu_{s+n} - \mu_n)}{\sqrt{\frac{\sigma_{s+n}^2 - \sigma_n^2}{2}}}$$

where μ_{s+n} and σ_{s+n}^2 are the mean and variance, respectively, of the response to the signal in noise, and μ_n and σ_n^2 are the mean and variance, respectively, of the response to noise alone. The measure d_a of Simpson and Fitter (1973) is similar to the more familiar d' (Green and Swets 1966), but it does not

assume equal variances in the distributions of amplitudes in response to signals in noise and noise alone. We fitted exponential curves to the d_a values for each signal location \times noise location condition using MATLAB's *fminsearch* function (Fig. 1C). Sigmoid fits were also considered, because it was at least possible that the tympanum response might "saturate," but exponential curve fits were ultimately chosen over sigmoid fits because they consistently produced higher R^2 values. The signal detection threshold was taken to be the lowest signal level along the fitted curve for which the interpolated response had a d_a value exceeding 2.0. These threshold measurements represent a useful tool for comparing responses of the tympanum to signals presented in noise under various conditions and should not be interpreted as behavioral or neural signal detection thresholds. We chose a threshold value of $d_a=2.0$ because laser measurements of the tympanum were extremely sensitive to the presence of the signal in all noise conditions. A threshold criterion closer to $d_a=1.0$ resulted in floor effects that made the data uninterpretable.

To compare responses across noise locations, we computed two measures of threshold difference. First, we computed differences in threshold for each angular separation between signal and noise relative to its respective co-located condition (signal/noise, 0/0°; +90/+90°; and -90/-90°). Second, we computed threshold differences relative to the condition in which noise was presented from directly in front of the animal (0°) without regard for signal location. Positive threshold differences (relative to either the co-located or the frontal noise conditions) indicate masking release and negative values indicate relatively greater masking.

Statistical Analysis

We analyzed absolute signal detection thresholds and our two measures of threshold differences in separate 3 (signal location) \times 12 (noise location or noise separation) repeated measures analyses of variance (ANOVAs). In all analyses, *signal location* (0, +90, -90°) and *noise location* are given relative to the orientation of the frog's snout (frontal=0°), with positive values indicating positions on the animal's right side (Fig. 1B). In our analysis of threshold differences relative to each co-located condition, *noise separation* is stated relative to the respective co-located condition, with positive and negative values indicating directions to the right and left of the signal speaker, respectively, as viewed facing the signal speaker. Hence, a value of -30° means the noise source was located 30° to the left of the specified signal location (e.g., -30° separation for signal/noise, 0/-30°; +90/+60°; or -90/-120°). For each ANOVA model, we used the Greenhouse and Geisser (1959)

method to correct P values for violations of sphericity. Our data met the other assumptions of parametric statistical tests (e.g., normality). We report partial η^2 as a measure of effect size for all main effects and interactions. SPSS version 21 was used for all statistical analyses, and we adopted a significance criterion of $\alpha=0.05$.

We explored the inclusion of subject sex as a between-subjects effect in these ANOVA models, but the main effects of sex ($0.067 < P < 0.575$) and all interactions including sex as a factor ($0.054 < P < 0.752$) were non-significant in all analyses. Therefore, we do not include subject sex in the analyses reported here. We also explored using mass, length, and interaural distance as mean-centered covariates. These size-dependent measures were significantly inter-correlated (two-tailed Pearson product-moment correlations: mass vs. length: $r=0.71$, $P=0.001$; mass vs. interaural distance: $r=0.49$, $P=0.046$; length vs. interaural distance: $r=0.70$, $P=0.001$). Inclusion of each size-dependent measure as a covariate in separate analysis of covariance (ANCOVA) models returned qualitatively similar outcomes. For analyses of signal detection thresholds, the main effect of a size-related covariate was significant or nearly so ($0.008 < P < 0.059$), but no two-way or three-way interactions with a covariate were significant ($0.144 < P < 0.930$). For analyses of threshold differences, the main effects of a size-related covariate, and all two-way and three-way interactions with the covariate, were non-significant ($0.125 < P < 0.972$). Therefore, we did not include any covariates in our final models. Instead, we performed a principal component analysis on standardized measures (z scores) of mass, length, and interaural distance and used linear regression to analyze the relationship between the grand mean of signal detection thresholds (averaged over signal and noise locations) and each principal component with an eigenvalue greater than 1.0.

RESULTS

Signal Detection Thresholds

Table 1 reports means and SDs for signal detection thresholds at all 36 combinations of signal location and noise location (both relative to the animal's snout). Figure 2A plots mean signal detection thresholds in the form of a polar plot, with the subject oriented toward 0° . There was considerable variability among individuals (as indicated by the size of the SDs reported in Table 1) compared with the magnitude of differences among means observed across treatments. It was primarily for this reason that we employed a large, within-subjects design, which is better able to reveal differences across treatments within individuals when there is a large degree of variation among

individuals. This issue of individual variability has not been apparent in most previous biophysical studies of frog tympana because those studies have typically used much smaller sample sizes compared to our study. In several cases, previous studies have presented data from only a single, representative individual for some analyses. We have purposefully taken a different approach that quantifies central tendencies and variability in a representative *sample* of individuals.

Signal detection thresholds varied significantly with both signal location and noise location (Table 2). The interaction between signal location and noise location was not significant (Table 2). Across all signal and noise locations, mean signal detection thresholds ranged from 58.8 ± 2.2 dB at the $+90^\circ$ signal location and -60° noise location to 68.3 ± 3.3 dB at the -90° signal location and $+120^\circ$ noise location (Table 1). Detection thresholds were lower when the signal was presented from the side of the animal ipsilateral ($+90^\circ$) to the measured tympanum, and higher when the signal was presented from the side of the animal contralateral (-90°) to the measured tympanum (Fig. 2A and Table 1). Irrespective of signal location, thresholds were generally higher when noise was presented in the hemifield ipsilateral to the measured tympanum (Fig. 2A and Table 1).

Subject body size was inversely related with signal detection thresholds. The principal component analysis returned one factor with an eigenvalue (2.3) greater than 1.0. This single factor explained 75.7% of the variance and was positively correlated with mass ($r=0.84$), length ($r=0.93$), and interaural distance ($r=0.84$). A linear regression of individual means of all signal detection thresholds, averaged across all signal and noise locations, on individual scores from the first principal component indicated a significantly negative relationship (Fig. 3, $\beta=-0.61$, adj. $R^2=0.35$, $F_{1, 15}=9.4$, $P=0.008$; $N=17$ individuals).

Threshold Differences Relative to Co-located Noise Conditions

Differences in threshold between the co-located and separated conditions are summarized as functions of absolute signal location and absolute noise location (relative to the animal's snout) in Table 1 and depicted as polar plots in Figure 2B. Threshold differences are plotted as 0 dB in the three co-located conditions of Figure 2B (signal/noise, $0/0^\circ$; $+90/+90^\circ$; and $-90/-90^\circ$). In statistical analyses of signal location and noise *separation* (relative to each co-located condition), threshold differences were influenced by a significant main effect of signal location and a significant two-way interaction between signal location and noise separation; the main effect of

TABLE 1

Means and standard deviations for absolute signal detection thresholds (means plotted in Fig. 2A), for the threshold differences relative to the co-located conditions (means plotted in Fig. 2B), and for the threshold differences relative to the frontal noise condition (means plotted in Fig. 2C).

Noise location	Absolute detection thresholds (dB)			Threshold differences relative to the co-located conditions (dB)			Threshold differences relative to the frontal noise conditions (dB)			Tympanum response difference in noise only relative to frontal noise (dB)
	0	+90	-90	0	+90	-90	0	+90	-90	
0	65.4 ± 3.4	62.2 ± 4.3	66.3 ± 2.8		0.6 ± 5.1	-1.7 ± 4.0				
+30	65.6 ± 5.6	63.0 ± 3.0	67.7 ± 2.1	-0.2 ± 4.4	-0.2 ± 2.7	-3.0 ± 3.1	-0.2 ± 4.4	-0.8 ± 5.1	-1.3 ± 3.3	-1.1 ± 0.4
+60	66.7 ± 5.4	61.9 ± 2.4	67.9 ± 2.9	-1.3 ± 4.7	1.0 ± 3.0	-3.2 ± 3.4	-1.3 ± 4.7	0.3 ± 4.7	-1.5 ± 3.9	-1.5 ± 0.6
+90	65.5 ± 4.2	62.8 ± 2.5	67.3 ± 3.1	-0.1 ± 2.6		-2.7 ± 3.2	-0.1 ± 2.6	-0.6 ± 5.1	-1.0 ± 3.8	-1.6 ± 0.7
+120	66.2 ± 3.8	63.2 ± 2.6	68.3 ± 3.3	-0.8 ± 2.7	-0.4 ± 2.9	-3.7 ± 3.3	-0.8 ± 2.7	-1.0 ± 4.5	-2.0 ± 3.9	-1.6 ± 0.9
+150	64.9 ± 4.3	63.0 ± 2.2	67.9 ± 3.8	0.5 ± 3.9	-0.1 ± 3.0	-3.3 ± 4.2	0.5 ± 3.9	-0.7 ± 4.1	-1.6 ± 3.9	-0.9 ± 1.2
+180	65.7 ± 4.1	62.4 ± 2.7	66.3 ± 3.0	-0.3 ± 3.1	0.5 ± 2.6	-1.6 ± 2.6	-0.3 ± 3.1	-0.1 ± 3.7	0.1 ± 3.5	-0.6 ± 1.1
-150	65.0 ± 5.0	62.5 ± 3.4	66.4 ± 3.9	0.4 ± 3.5	0.3 ± 3.5	-1.7 ± 2.7	0.4 ± 3.5	-0.3 ± 5.4	0.0 ± 4.4	0.1 ± 1.4
-120	63.3 ± 3.7	60.2 ± 4.0	65.4 ± 3.2	2.0 ± 3.7	2.6 ± 4.9	-0.8 ± 3.3	2.0 ± 3.7	2.0 ± 4.5	0.9 ± 4.2	1.3 ± 1.3
-90	62.5 ± 5.2	60.2 ± 3.8	64.6 ± 2.9	2.8 ± 3.6	2.6 ± 5.1		2.8 ± 3.6	2.0 ± 3.5	1.7 ± 4.0	2.2 ± 1.1
-60	62.8 ± 4.3	58.8 ± 2.2	64.4 ± 4.1	2.6 ± 4.5	4.0 ± 3.7	0.2 ± 3.8	2.6 ± 4.5	3.4 ± 3.4	1.9 ± 4.7	1.9 ± 0.5
-30	64.2 ± 3.1	59.5 ± 2.2	64.0 ± 3.3	1.2 ± 2.4	3.3 ± 3.7	0.6 ± 3.7	1.2 ± 2.4	2.7 ± 5.0	2.3 ± 3.6	1 ± 0.3

Thresholds and threshold differences are shown for three signal locations (0, +90, and -90°) and 12 noise locations. Also shown are differences in the tympanum's amplitude response in the noise only condition relative to frontal noise (red line in Fig. 2C).

noise separation was not significant (Table 2). Threshold differences as a function of noise separation were largest in the +90° signal location (i.e., signal ipsilateral to the measured tympanum; blue line in Fig. 2B) and smallest in the -90° signal location (i.e., signal contralateral to the measured tympanum; gray line in Fig. 2B). Across all 36 combinations of signal location and noise separation, the mean magnitude of SRM ranged between 0.2 ± 3.8 dB, at the -90° signal location, and +30° noise separation (i.e., -60° noise location; Table 1 and Fig. 2B), to a maximum of 4.0 ± 3.7 dB at the +90° signal location and -150° noise separation (i.e., -60° noise location; Table 1 and Fig. 2B). At several combinations of signal location and noise separation, masking actually increased relative to the co-located condition (as indicated by negative values in Table 1). This additional masking was largest when the signal was presented contralateral to the measured tympanum (-90°), and noise was presented in the hemifield ipsilateral to the measured tympanum (between 0 and +180°).

Threshold Differences Relative to Frontal Noise Conditions

To evaluate the hypothesis that threshold differences in various spatial configurations of signal and noise result from the tympanum's directionality, we computed threshold differences for each signal location relative to the condition in which the noise was presented directly in front of the animal (0°; Fig. 2C). If tympanum directionality alone determines the magnitude of SRM, then the directionality of threshold differences relative to a fixed noise position (0° in this case) should depend

strongly on differences in noise location but be largely independent of signal location. In addition, the pattern of threshold differences observed as a function of noise location, relative to the frontal noise condition, should be similar to those observed when noise was presented in the absence of a signal. The data were consistent with both of these expectations.

Noise location had a significant effect on threshold differences measured relative to the frontal noise condition, but the main effect of signal location and the signal location × noise location interaction were not significant (Table 2). Averaged across subjects, mean threshold differences relative to the frontal noise condition ranged between -2.0 ± 3.9 and 3.4 ± 3.4 dB across all signal and noise locations (Table 1 and Fig. 2C). Threshold differences were generally greater in the frontal hemifield to the side of the animal contralateral to the measured tympanum (Fig. 2C). The maximum threshold differences relative to the frontal noise condition ranged between 2.3 ± 3.6 and 3.4 ± 3.4 dB across the three signal locations. Averaged across individuals and signal locations, the maximum threshold difference between any two noise locations was 4.3 dB and was similar for presentations from all three signal locations (0° signal, 4.1 ± 5.0 dB; +90° signal, 4.3 ± 3.3 dB; -90° signal, 4.3 ± 3.6 dB).

The pattern of threshold differences relative to a frontal noise closely followed the directionality observed in the tympanum's response to noise alone. In the noise alone condition (Table 1 and red line in Fig. 2C), mean threshold differences across noise locations, relative to the frontal noise condition, ranged between -1.6 ± 0.7

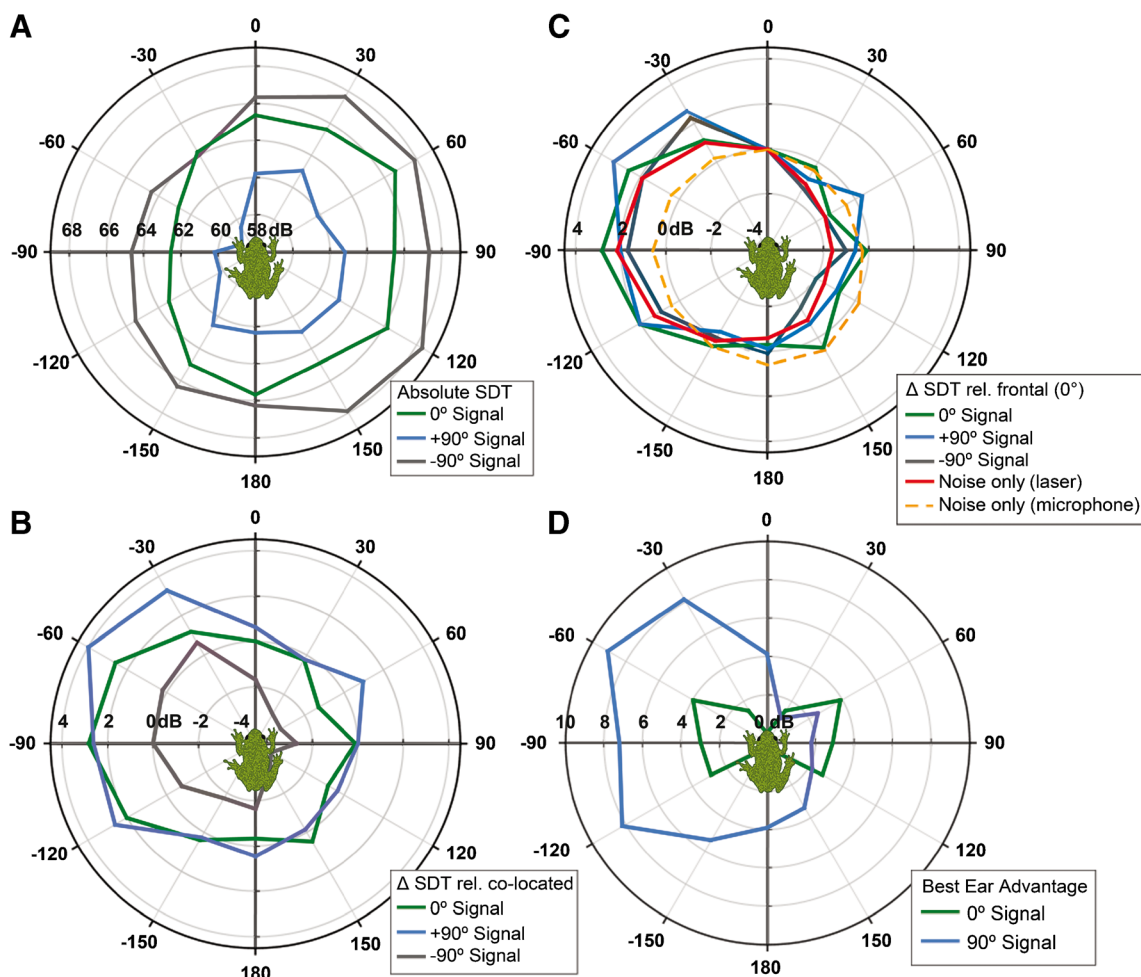


FIG. 2. Polar plots showing mean signal detection thresholds (SDT) or threshold differences (Δ SDT). All plots show data measured from the right tympanum for the absolute signal and noise locations indicated in azimuth around a subject with its snout oriented toward 0° (frontal). Distances along the radial axes correspond to thresholds or threshold differences measured in dB. **A** Mean signal detection thresholds in response to calls broadcast from three signal locations (0, +90, and -90°; see text) in the presence of chorus-like noise broadcast from 12 different azimuthal angles (0 to 330°, 30° steps; plotted on the angular axis). **B** SRM depicted as the mean differences in signal detection thresholds as functions of signal location and noise location computed relative to the three co-located conditions (signal/noise, 0/0°; +90/+90°; and -90/-90°). **C** Mean differences

in signal detection thresholds as functions of signal location and noise location computed relative to the frontal noise presented at 0° (signal/noise, 0/0°; +90/0°; and -90/0°). Also plotted are the amplitude of tympanum vibrations and sound pressure level adjacent to the right tympanum in response to noise alone after also standardizing these values to their magnitude at the 0° noise location. In **B** and **C**, positive values indicate masking release and negative values indicate greater masking relative to the co-located conditions (in **B**) and the frontal noise condition (in **C**). **D** Mean best-ear advantage as functions of signal location and noise location. Values were calculated from measurements taken at the right tympanum, assuming bilateral symmetry in the mechanical response of the two tympana.

and 2.2 ± 1.1 dB when averaged across individuals. Similar to the pattern of threshold differences relative to the frontal noise condition, differences in response to noise alone relative to the frontal noise condition were greatest in the frontal hemifield to the side of the animal contralateral to the measured tympanum (Fig. 2C). Across individuals, the maximum directionality in the response to noise alone averaged 3.8 ± 0.9 dB in pairwise comparisons across all noise locations (cf. 4.3 dB for differences in signal detection thresholds relative to the frontal noise condition). Notably, the maximum differences in the SPL of the noise measured with a probe

microphone adjacent to the tympanum ipsilateral to the laser were considerably lower, with a mean of 1.1 ± 0.4 dB, highlighting the contribution of internal coupling between the two ears to directionality in the response of the tympanum.

Best-Ear Advantage for Internally Coupled Ears

The best ear for listening for a signal in noise is the one with the higher SNR ratio. In considering a best-ear advantage for frogs, it must be understood that this

TABLE 2

Results of factorial repeated measures ANOVAs examining the effects of signal location and noise location on the mean signal detection thresholds plotted in Figure 2A and the mean threshold differences plotted in Figure 2C and the effects of signal location and noise separation on the mean threshold differences plotted in Figure 2B

Response variable	Factor	df	F	P	Partial η^2
Signal detection thresholds	Signal location	2, 32	18.6	<0.001	0.54
	Noise location	11, 176	11.9	<0.001	0.43
	Signal location \times noise location	22, 352	0.6	0.702	0.05
Threshold differences relative to co-located	Signal location	2, 32	8.5	0.002	0.35
	Noise separation	11, 176	1.8	0.129	0.10
	Signal location \times noise separation	22, 352	6.2	<0.001	0.28
	Signal location	2, 32	0.2	0.761	0.01
Threshold differences relative to frontal noise	Noise location	11, 176	11.9	<0.001	0.43
	Signal location \times noise location	22, 352	0.8	0.641	0.05

advantage is not strictly a monaural cue, as it is in mammals. This is because in frogs, and in other tetrapod vertebrates having internally coupled ears, any “best-ear” advantage necessarily relies not only on input to the external surface of the tympanum but also on that to the tympanum’s internal surface provided via the internal coupling itself. We computed the best-ear advantage as a function of noise location for the 0° (frontal) and +90° (ipsilateral) signal locations. To do so, we assumed bilateral symmetry and subtracted the assumed threshold SNR for the contralateral ear (folded over the midline) from that measured for the tympanum ipsilateral to the laser (see Fig. 2D). For example, to compute the best-ear

advantage for the +90° signal location and the -30° noise location, we computed the threshold difference between the two signal/noise locations of +90/+30° and +90/-30°. Similar procedures have been used previously to measure interaural vibration amplitude differences (IVAD) in studies of the directionality of frog ears (e.g., Jørgensen and Gerhardt 1991; Ho and Narins 2006). Our general expectation was that the magnitude of a best-ear advantage should be about 8.6 dB or less because it should approach twice the maximum threshold difference measured between any two noise locations (4.3 dB). Furthermore, given the tympanum’s bilaterally symmetrical cardioid pattern of directionality, we expected the best-ear advantage would be larger when signals originated from a lateral position (+90°) compared with a frontal position (0°).

The best-ear advantage varied with both signal location and noise location (Fig. 2D). When the signal location was +90° (ipsilateral to the measured tympanum), the ear closest to the signal source had the lowest detection thresholds and was the best ear for listening at all noise locations. At this signal location (+90°), the mean best-ear advantage ranged between 1.0 ± 4.1 dB (at the +30° noise location) and 9.0 ± 3.7 dB (at the -60° noise location) (blue line in Fig. 2D). The maximum value of 9.0 dB is close to the expected maximum best-ear advantage of 8.6 dB. For frontal signal presentations (0°), the ear furthest from the noise source was the best ear for listening at all noise locations, and the mean best-ear advantage ranged between 0 dB along the midline and 3.9 ± 3.7 dB at the $\pm 60^\circ$ noise locations (green line in Fig. 2D).

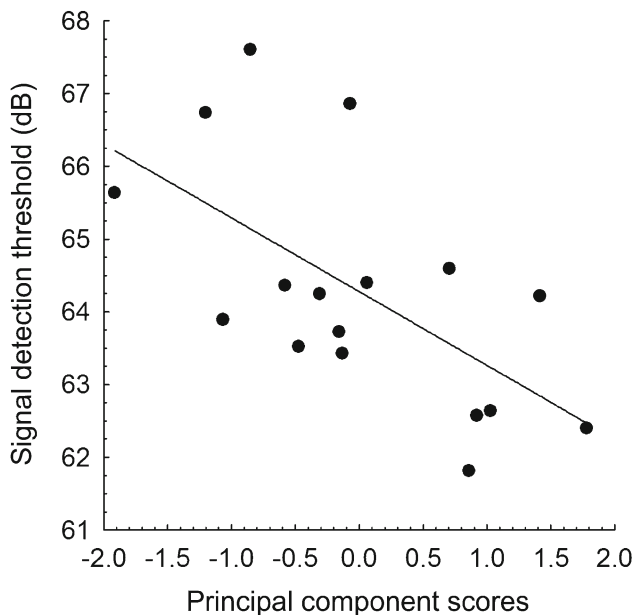


FIG. 3. Relationship between body size and signal detection thresholds. The scatterplot shows the best-fit regression line for the relationship between the individual means of signal detection thresholds (averaged across signal and noise locations within each individual) and individual scores on the first principal component from a principal component analysis of three body size measures (mass, length, and interaural distance).

DISCUSSION

Treefrogs in the genus *Hyla* represent a group of nonhuman vertebrates for which several behavioral studies have measured the benefits of SRM (reviewed in Bee 2012, 2015). Spatial separation between

advertisement calls and noise reduces the time required for phonotaxis to a source of calls (Bee 2007), reduces signal recognition thresholds (Schwartz and Gerhardt 1989; Nityananda and Bee 2012), improves discrimination between the calls of conspecific and heterospecific males (Bee 2008; Ward et al. 2013a), and improves discrimination between different conspecific males (Richardson and Lengagne 2010), though not between different conspecific call types (Schwartz and Gerhardt 1989). In the environment of a chorus, these improvements in performance could yield benefits in terms of evolutionary fitness, ranging from reduced exposure to predators to reduced errors in mating decisions. Current estimates for the magnitude of SRM from behavioral studies of treefrogs vary between 3 and 12 dB.

Our aim in this study was to evaluate the contribution of the auditory periphery to SRM by testing the hypothesis that the inherent directionality of the treefrog's internally coupled ears determines the pattern and magnitude of SRM in the amplitude of the tympanum's response. Three lines of evidence support this hypothesis. First, detection thresholds varied independently with *absolute* signal location and with *absolute* noise location (each measured relative to the snout of the frog) but did not depend on an interaction between signal and noise location (Fig. 2A). Second, when threshold differences were measured relative to co-located conditions, they depended both on absolute signal location and an interaction between signal location and noise separation (Fig. 2B). However, when threshold differences were instead standardized relative to the frontal noise condition, they varied only according to absolute noise location around the animal and were again independent of signal location (Fig. 2C). Finally, spatial variation in the magnitude of threshold differences closely followed the tympanum's inherent directional response to a single sound source (Fig. 2C). Moreover, the maximum threshold differences observed when calls and noise were presented simultaneously from different locations (4.1 to 4.3 dB) were very similar to the mean magnitudes of maximum directionality observed when either noise (3.8 dB, this study) or calls (3.9 dB; Caldwell et al. 2014) were presented alone as a single source. Together, these patterns of results indicate that the effects of variation in noise location on the tympanum's response to a spatially separated signal were largely independent of the absolute location of the signal and were of a magnitude predicted by the tympanum's directional response to a single sound source.

The improvement in detection thresholds we observed with spatial separation between signals and noise relative to a co-located condition (SRM up to 4.0 dB) is on par with previously reported measurements of SRM at the level of the frog auditory nerve. Lin and Feng (2001) measured SRM in the spiking activity of auditory nerve fibers in northern leopard frogs, *Rana (Lithobates) pipiens*, in response to free-field presentations of a mating call in the presence of masking noise. Neural signal detection thresholds were compared between a co-located condition and signal-noise separations of up to 180°. Averaged across units, the maximum SRM was 2.9 ± 2.8 dB (ranging up to 9 dB). Thus, the magnitudes of SRM reported in the present study fall within the range of values reported for the frog auditory nerve.

The magnitude of neural SRM increases in the anuran central auditory system compared with that observed at the periphery. Lin and Feng (2001) also measured SRM in the spiking activity of neurons in the anuran inferior colliculus (IC), a midbrain nucleus with important functions in processing vocal communication sounds (Bass et al. 2005; Rose and Gooler 2007; Wilczynski and Ryan 2010). On average, the maximum SRM exhibited by IC neurons was 9.4 ± 8.0 dB (ranging up to 43 dB), and SRM in the IC was significantly greater than that observed in auditory nerve responses (see also Ratnam and Feng 1998). Lin and Feng (2003) later showed that the greater SRM observed centrally is brought about, at least in part, by binaural computations in the midbrain based on GABAergic inhibition and spatial tuning. Interestingly, the magnitude of SRM exhibited by frog IC neurons is quite close to the maximum best-ear advantage of 9 dB reported in the present study. Recall that the best-ear advantage was computed as the difference in detection thresholds between the two ears for a given signal-noise separation. Hence, our data illustrate how the information necessary for binaural comparisons by the central auditory system is likely already present at the level of the periphery and originates with the inherent directionality of the frog's internally coupled ears.

Two studies of Cope's gray treefrog (*H. chrysocelis*) have yielded behavioral estimates of SRM in line with data reported in the present study for the same species. Nityananda and Bee (2012) measured signal recognition thresholds (sensu Bee and Schwartz 2009) when advertisement calls were co-located with chorus-like noise or separated by 90°. Thresholds were lower in the separated condition on about 70% of trials, with an average SRM of 4.5 dB. This behavioral estimate of SRM is similar to the maximum SRM observed in the present study (4.0 dB). Hence, the magnitude of SRM based on differences in behavioral thresholds was similar to that observed for detection

thresholds measured biophysically (this study) and electrophysiologically (Lin and Feng 2001), suggesting a tight linkage between signal detection and signal recognition in frogs.

In an earlier study of Cope's gray treefrogs, Bee (2007) estimated SRM between co-located and 90° separated conditions to be somewhat higher, between 6 and 12 dB. This estimate was based not on differences in behavioral thresholds but on differences in the time required for females to complete their phonotactic approach toward a source of calls located 1 m away. Like other treefrogs (Feng et al. 1976; Rheinlaender et al. 1979), females of this species often exhibit a stereotypical zigzag pattern of phonotaxis toward a source of calls (Caldwell and Bee 2014). The off-axis listening that results from such an approach potentially improves source localization by maximizing binaural disparities. It might also provide a way for listeners to exploit their best-ear advantage when multiple sound sources are active concurrently. In the present study, the angular pattern and magnitude of best-ear advantage varied markedly with signal location and was much greater (and more asymmetrical) when signals were presented from a lateral position (up to 9 dB) compared with directly in front of the animal (up to 3.9 dB). A zigzag phonotactic approach, or off-axis listening more generally, in the presence of concurrent but spatially separated sounds might allow females to optimally exploit the directionality of their best-ear advantage while approaching a source of calls in noise. Notably, the midpoint of the range of SRM of 6 to 12 dB reported by Bee (2007) based on phonotaxis latencies falls precisely at the maximum best-ear advantage reported in the present study.

Although many insects and most tetrapod vertebrates have ears that are internally coupled, we still know very little about how such ears function in the perceptual analysis of noisy and complex acoustic scenes. The present study provides one vital piece of this larger puzzle. We believe treefrogs and orthopteran insects are among the best groups of animals for more in-depth investigations into these questions, because they have internally coupled ears and use them to solve biological analogues of the human cocktail party problem (McDermott 2009; Römer 2013; Vélez et al. 2013; Bee 2015). A deeper understanding of how internally coupled ears process spatial cues in the analysis of acoustic scenes will emerge by integrating biomechanical, neurophysiological, and behavioral studies within the same species and in more naturalistic listening conditions (Römer 2015). In turn, improved understanding of how internally coupled ears contribute to processing sounds in complex acoustic scenes might have translational benefits related to better microphone designs in hearing aids (Michelsen and Larsen 2008).

ACKNOWLEDGMENTS

We thank Katrina Schrode for providing code used in data analysis, Jessica Ward for logistical support, Shelby Seckora, Nathan Buerkle, and Sam Levin for assistance in data collection, and three anonymous reviewers for helpful feedback on earlier drafts. This research was supported by a grant from the National Institute on Deafness and Other Communication Disorders (R01 DC009582).

COMPLIANCE WITH ETHICAL STANDARDS

Conflicts of Interest The authors declare that they have no conflicts of interest.

REFERENCES

- BASS AH, ROSE GJ, PRITZ MB (2005) Auditory midbrain of fish, amphibians, and reptiles: model systems for understanding auditory function. In: *The inferior colliculus*, pp 459–492: Springer.
- BEE MA (2007) Sound source segregation in grey treefrogs: spatial release from masking by the sound of a chorus. *Anim Behav* 74:549–558
- BEE MA (2008) Finding a mate at a cocktail party: spatial release from masking improves acoustic mate recognition in grey treefrogs. *Anim Behav* 75:1781–1791
- BEE MA (2012) Sound source perception in anuran amphibians. *Curr Opin Neurobiol* 22:301–310
- BEE MA (2015) Treefrogs as animal models for research on auditory scene analysis and the cocktail party problem. *Int J Psychophysiol* 95:216–237
- BEE MA, MICHEYL C (2008) The cocktail party problem: what is it? How can it be solved? And why should animal behaviorists study it? *J Comp Psychol* 122:235–251
- BEE MA, SCHWARTZ JJ (2009) Behavioral measures of signal recognition thresholds in frogs in the presence and absence of chorus-shaped noise. *J Acoust Soc Am* 126:2788–2801
- BRONKHORST AW (2000) The cocktail party phenomenon: a review of research on speech intelligibility in multiple-talker conditions. *Acustica* 86:117–128
- BRONKHORST AW, PLOMP R (1988) The effect of head-induced interaural time and level differences on speech intelligibility in noise. *J Acoust Soc Am* 83:1508–1516
- BRUMM H (ED) (2013) *Animal communication and noise*. Springer, New York
- BUEKLE NP, SCHRODE KM, BEE MA (2014) Assessing stimulus and subject influences on auditory evoked potentials and their relation to peripheral physiology in green treefrogs (*Hyla cinerea*). *Comp Biochem Physiol A* 178:68–81
- CAIRD D, PILLMANN F, KLINKE R (1989) Responses of single cells in the cat inferior colliculus to binaural masking level difference signals. *Hear Res* 43:1–23
- CALDWELL MS, BEE MA (2014) Spatial hearing in Cope's gray treefrog: I. Open and closed loop experiments on sound localization in the presence and absence of noise. *Journal of Comparative Physiology A* 200:265–284
- CALDWELL MS, LEE N, SCHRODE KM, JOHNS AR, CHRISTENSEN-DALSGAARD J, BEE MA (2014) Spatial hearing in Cope's gray treefrog: II. Frequency-dependent directionality in the amplitude and phase of tympanum vibrations. *Journal of Comparative Physiology A* 200:285–304

- CHRISTENSEN-DALSGAARD J (2005) Directional hearing in nonmammalian tetrapods. In: Popper AN, Fay RR (eds) Sound source localization. Springer, New York, pp 67–123
- CHRISTENSEN-DALSGAARD J (2011) Vertebrate pressure-gradient receivers. *Hear Res* 273:37–45
- DENT ML, McCLAIN EM, BEST V, OZMERAL E, NARAYAN R, GALLUN FJ, SEN K, SHINN-CUNNINGHAM BG (2009) Spatial unmasking of birdsong in zebra finches (*Taeniopygia guttata*) and budgerigars (*Melopsittacus undulatus*). *J Comp Psychol* 123:357–367
- EHRET G, TAUTZ J, SCHMITZ B, NARINS PM (1990) Hearing through the lungs: lung-eardrum transmission of sound in the frog *Eleutherodactylus coqui*. *Naturwissenschaften* 77:192–194
- FENG AS, GERHARDT HC, CAPRANICA RR (1976) Sound localization behavior of the green treefrog (*Hyla cinerea*) and the barking treefrog (*Hyla gratiosa*). *J Comp Physiol* 107:241–252
- GERHARDT HC (2001) Acoustic communication in two groups of closely related treefrogs. *Adv Study Behav* 30:99–167
- GERHARDT HC, HUBER F (2002) Acoustic communication in insects and anurans: common problems and diverse solutions. Chicago University Press, Chicago
- GREEN DM, SWETS JA (1966) Signal detection theory and psychophysics. John Wiley & Sons, New York
- GREENHOUSE SW, GEISSER S (1959) On methods in the analysis of profile data. *Psychometrika* 24:95–112
- HINE JE, MARTIN RL, MOORE DR (1994) Free-field binaural unmasking in ferrets. *Behav Neurosci* 108:196–205
- HO CCK, NARINS PM (2006) Directionality of the pressure-difference receiver ears in the northern leopard frog, *Rana pipiens pipiens*. *J Comp Physiol A* 192:417–429
- HOLT MM, SCHUSTERMAN RJ (2007) Spatial release from masking of aerial tones in pinnipeds. *J Acoust Soc Am* 121:1219–1225
- ISON JR, AGRAWAL P (1998) The effect of spatial separation of signal and noise on masking in the free field as a function of signal frequency and age in the mouse. *J Acoust Soc Am* 104:1689–1695
- JØRGENSEN MB (1991) Comparative studies of the biophysics of directional hearing in anurans. *J Comp Physiol A* 169:591–598
- JØRGENSEN MB, GERHARDT HC (1991) Directional hearing in the gray tree frog *Hyla versicolor*: eardrum vibrations and phonotaxis. *J Comp Physiol A* 169:177–183
- JØRGENSEN MB, SCHMITZ B, CHRISTENSEN-DALSGAARD J (1991) Biophysics of directional hearing in the frog *Eleutherodactylus coqui*. *J Comp Physiol A* 168:223–232
- LIN WY, FENG AS (2001) Free-field unmasking response characteristics of frog auditory nerve fibers: comparison with the responses of midbrain auditory neurons. *J Comp Physiol A* 187:699–712
- LIN WY, FENG AS (2003) GABA is involved in spatial unmasking in the frog auditory midbrain. *J Neurosci* 23:8143–8151
- McDERMOTT JH (2009) The cocktail party problem. *Curr Biol* 19:R1024–R1027
- MICHELSSEN A, LARSEN ON (2008) Pressure difference receiving ears. *Bioinspir Biomim* 3:011001
- NARINS PM (1995) Frog communication. *Sci Am* 273:78–83
- NITYANANDA V, BEE MA (2011) Finding your mate at a cocktail party: frequency separation promotes auditory stream segregation of concurrent voices in multi-species frog choruses. *PLoS One* 6, e21191
- NITYANANDA V, BEE MA (2012) Spatial release from masking in a free-field source identification task by gray treefrogs. *Hear Res* 285:86–97
- PTACEK MB, GERHARDT HC, SAGE RD (1994) Speciation by polyploidy in treefrogs: multiple origins of the tetraploid, *Hyla versicolor*. *Evolution* 48:898–908
- RATNAM R, FENG AS (1998) Detection of auditory signals by frog inferior collicular neurons in the presence of spatially separated noise. *J Neurophysiol* 80:2848–2859
- RHEINLAENDER J, GERHARDT HC, YAGER DD, CAPRANICA RR (1979) Accuracy of phonotaxis by the green treefrog (*Hyla cinerea*). *J Comp Physiol* 133:247–255
- RICHARDSON C, LENGAGNE T (2010) Multiple signals and male spacing affect female preference at cocktail parties in treefrogs. *Proc R Soc B-Biol Sci* 277:1247–1252
- ROBERT D (2005) Directional hearing in insects. In: Popper AN, Fay RR (eds) Sound source localization. Springer, New York, NY, pp 6–35
- RÖMER H (2013) Masking by noise in acoustic insects: problems and solutions. In: Brumm H (ed) Animal communication and noise. Springer, New York, pp 33–63
- RÖMER H (2015) Directional hearing: from biophysical binaural cues to directional hearing outdoors. *J Comp Physiol A* 201:87–97
- ROSE GJ, GOOLER DM (2007) Function of the amphibian central auditory system. In: Narins PA, Feng AS, Fay RR, Popper AN (eds) Hearing and sound communication in amphibians. Springer, New York, pp 250–290
- SCHMIDT AKD, RÖMER H (2011) Solutions to the cocktail party problem in insects: selective filters, spatial release from masking and gain control in tropical crickets. *PLoS One* 6, e28593
- SCHWARTZ JJ, GERHARDT HC (1989) Spatially mediated release from auditory masking in an anuran amphibian. *J Comp Physiol A* 166:37–41
- SIMPSON AJ, FITTER MJ (1973) What is the best index of detectability? *Psychol Bull* 80:481–488
- VÉLEZ A, SCHWARTZ JJ, BEE MA (2013) Anuran acoustic signal perception in noisy environments. In: Brumm H (ed) Animal communication and noise. Springer, New York, pp 133–185
- WARD JL, BUERKLE NP, BEE MA (2013a) Spatial release from masking improves sound pattern discrimination along a biologically relevant pulse-rate continuum in gray treefrogs. *Hear Res* 306:63–75
- WARD JL, LOVE EK, VÉLEZ A, BUERKLE NP, O'BRYAN LR, BEE MA (2013b) Multitasking males and multiplicative females: dynamic signalling and receiver preferences in Cope's grey treefrog. *Anim Behav* 86:231–243
- WARNECKE M, BATES ME, FLORES V, SIMMONS JA (2014) Spatial release from simultaneous echo masking in bat sonar. *J Acoust Soc Am* 135:3077–3085
- WILCZYNSKI W, RYAN MJ (2010) The behavioral neuroscience of anuran social signal processing. *Curr Opin Neurobiol* 20:754–763
- WILEY RH (2015) Noise matters: the evolution of communication. Harvard University Press, Cambridge, MA
- ZUREK PM (1992) Binaural advantages and directional effects in speech intelligibility. In: Studebaker GA, Hochberg I (eds) Acoustical factors affecting hearing aid performance. Allyn and Bacon, Boston, pp 255–276